Available online at www.sciencedirect.com
SCIENCE DIRECT®
Journal of Membrane Science 230 (2004) 13–19
journal of MEMBRANE SCIENCE
www.elsevier.com/locate/memsci

Influence of channel-width ratio on solvent extraction through a double-pass parallel-plate membrane module

H.M. Yeh*, C.H. Chen, T.Y. Yueh

Department of Chemical Engineering, Tamkang University, Tamsui 251, Taiwan, ROC

Received 10 January 2003; received in revised form 17 September 2003; accepted 30 September 2003

Abstract

The effect of the location of an impermeable barrier, which is placed for double pass in the raffinate phase, on solvent extraction through a parallel-plate membrane module, has been investigated. Theoretical predictions are in fairly good agreement with the experimental results. Considerable improvement in performance is obtainable if the subchannel width, as well as the mass-transfer area, of concurrent flow is as large as possible than that of concurrent flow, especially for low flow rate operation. It has been also checked that the hydraulic dissipated power due to the friction loss of fluid flow is very small and generally, the operating cost in all devices may be ignored.

Keywords: Membrane extraction; Double pass; Channel-width ratio

1. Introduction

Applications of the recycle-effect concept to the design and operation of the equipment with external or internal refluxes can effectively increase in fluid velocity and enhance the effect on heat and mass transfer, leading to improved performance [1–11]. Recently, the recycle effect on solvent extraction in microporous-membrane modules has been studied both theoretically and experimentally [12,13]. It was reported that extraction performance increases with the reflux ratio. However, operation at high reflux ratio might not compensate for the loss of hydraulic dissipated power. An alternate method for increasing fluid velocity by arranging a double flow operation in the membrane module with the impermeate barrier location adjustable. It is the purpose of this work to investigate the influence of width ratio of flow subchannels in the raffinate phase on solvent extraction through a double-pass parallel-plate membrane module.

2. Theory

Membrane extraction is carried out in a microporous-membrane device, in which the membrane is generally contacted with two immiscible fluids at two sides (phases a and b). However, if these two fluids are miscible, then the pores of the membrane is filled with another fluid (phase c) which is immiscible with these two fluids. The solute is extracted from phase a to phase c and then to phase b, or vice versa. This new technique overcomes the limitations of conventional liquid extraction, such as flooding, intimate mixing, limitations on independent phases flow rate variations, requirement of density difference and inability to handle particulates [14].

2.1. Governing equations

Fig. 1 shows the double-pass parallel-plate membrane extractor. An impermeable plate with negligible thickness is placed vertically to the upper plate and the membrane sheet to divide the channel into two subchannels (subchannels a_1 and a_2) of widths Δw and $(1-\Delta)w$. Thus, in the raffinate phase (phase a), the inlet fluid of volume rate and concentration $C_{a,i}$ flows steadily as well as cocurrently first and then countercurrently within subchannels a_1 and a_2, respectively. The extract phase (phase b) with inlet volume rate Q_b and concentration $C_{b,i}$ flows steadily through channel *b*. The assumptions made in this analysis are steady stats, no chemical reactions, uniform concentrations and velocities over the flow cross-sections, constant flow rates, constant mass-transfer coefficients and constant distribution coefficients.

* Corresponding author. Tel.: +886-2-9180149; fax: +886-2-26203887.
E-mail address: hmyeh@mail.tku.edu.tw (H.M. Yeh).

0376-7388/$ – see front matter © 2003 Elsevier B.V. All rights reserved.
doi:10.1016/j.memsci.2003.09.018

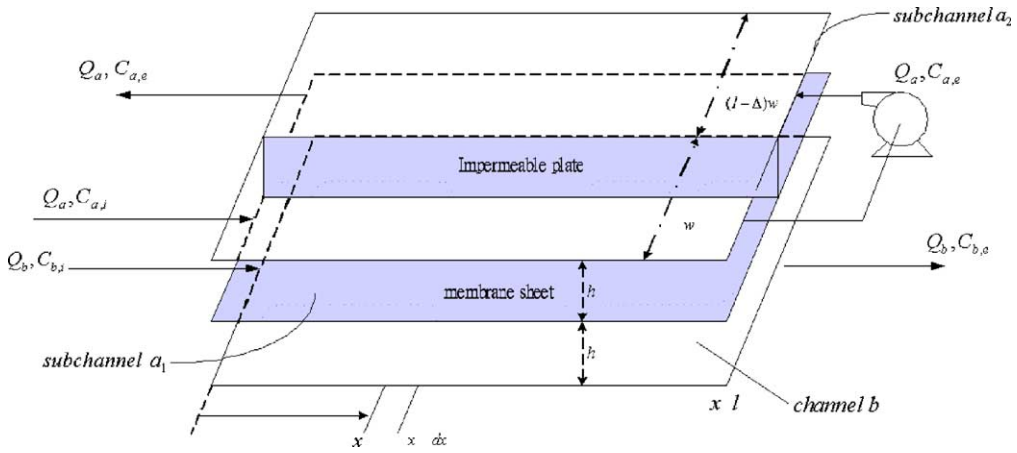

Fig. 1. Schematic diagram of double-pass parallel-plate membrane extractors.

Referring to Fig. 1, the mass balance over the right-hand section of the membrane extractor operated is

$$Q_{\mathrm{b}}(C_{\mathrm{b,e}} - C_{\mathrm{b}}) = Q_{\mathrm{a}}(C_{\mathrm{a},1} - C_{\mathrm{a},2}) \tag{1}$$

or

$$C_{\mathrm{b}} = C_{\mathrm{b,e}} - \left(\frac{Q_{\mathrm{a}}}{Q_{\mathrm{b}}}\right)(C_{\mathrm{a},1} - C_{\mathrm{a},2}) \tag{2}$$

Considering the mass transfer on subchannels a_1 and a_2 over the length dx:

$$-Q_{\mathrm{a}}\,\mathrm{d}C_{\mathrm{a},1} = K_1 \Delta w(H_{\mathrm{ac}}C_{\mathrm{a},1} - H_{\mathrm{bc}}C_{\mathrm{b}})\,\mathrm{d}x \tag{3}$$

$$Q_{\mathrm{a}}\,\mathrm{d}C_{\mathrm{a},2} = K_2(1-\Delta)w(H_{\mathrm{ac}}C_{\mathrm{a},2} - H_{\mathrm{bc}}C_{\mathrm{b}})\,\mathrm{d}x \tag{4}$$

where K_1 and K_2 are the overall mass-transfer coefficients in subchannels a_1 and a_2, respectively, while H_{ac} and H_{bc} are the distribution coefficients between two different phases, as defined by

$$H_{\mathrm{ac}} = \frac{\text{solute concentration in phase c}}{\text{solute concentration in phase a}} \tag{5}$$

Substituting the value of C_{b} from Eq. (2) into Eqs. (3) and (4), one obtains

$$\frac{\mathrm{d}C_{\mathrm{a},1}}{\mathrm{d}x} + \zeta C_{\mathrm{a},1} + \phi C_{\mathrm{a},2} = \xi C_{\mathrm{b,e}} \tag{6}$$

$$\frac{\mathrm{d}C_{\mathrm{a},2}}{\mathrm{d}x} + \omega C_{\mathrm{a},2} + \eta C_{\mathrm{a},1} = \theta C_{\mathrm{b,e}} \tag{7}$$

where

$$\zeta = K_1 \Delta w\left[\frac{H_{\mathrm{ac}}}{Q_{\mathrm{a}}} + \frac{H_{\mathrm{bc}}}{Q_{\mathrm{b}}}\right] \tag{8}$$

$$\phi = -\left(\frac{K_1 \Delta w H_{\mathrm{bc}}}{Q_{\mathrm{b}}}\right) \tag{9}$$

$$\xi = \left(\frac{K_1 \Delta w H_{\mathrm{bc}}}{Q_{\mathrm{a}}}\right) \tag{10}$$

$$\omega = -K_2(1-\Delta)w\left[\frac{H_{\mathrm{ac}}}{Q_{\mathrm{a}}} - \frac{H_{\mathrm{bc}}}{Q_{\mathrm{b}}}\right] \tag{11}$$

$$\eta = -K_2(1-\Delta)w\left(\frac{H_{\mathrm{bc}}}{Q_{\mathrm{b}}}\right) \tag{12}$$

$$\theta = -K_2(1-\Delta)w\left(\frac{H_{\mathrm{bc}}}{Q_{\mathrm{a}}}\right) \tag{13}$$

2.2. Concentration distributions

Eqs. (6) and (7) can be solved simultaneously for solute concentrations, $C_{\mathrm{a},1}$ and $C_{\mathrm{a},2}$, in subchannels a_1 and a_2 with the following boundary conditions:

$$\text{At } x = l: \quad C_{\mathrm{a},1} = C_{\mathrm{a},2} = C'_{\mathrm{a,e}} \tag{14}$$

The results are

$$C_{\mathrm{a},1} = \alpha\,\mathrm{e}^{\lambda_{\mathrm{a}}x} + \beta\,\mathrm{e}^{\lambda_{\mathrm{b}}x} + fC_{\mathrm{b,e}} \tag{15}$$

$$C_{\mathrm{a},2} = \frac{1}{\phi}[-(\lambda_{\mathrm{a}} + \zeta)\alpha\,\mathrm{e}^{\lambda_{\mathrm{a}}x} - (\lambda_{\mathrm{b}} + \zeta)\beta\,\mathrm{e}^{\lambda_{\mathrm{b}}x} + (\xi - \zeta f)C_{\mathrm{b,e}}] \tag{16}$$

where

$$\lambda_{\mathrm{a}} = \tfrac{1}{2}\left(-(\zeta+\omega) + \sqrt{(\zeta-\omega)^2 + 4\phi\eta}\right) \tag{17}$$

$$\lambda_{\mathrm{b}} = \tfrac{1}{2}\left(-(\zeta+\omega) - \sqrt{(\zeta-\omega)^2 + 4\phi\eta}\right) \tag{18}$$

$$f = \frac{\omega\xi - \phi\theta}{\zeta\omega - \phi\eta} \tag{19}$$

while α and β are the integration constants which are determined by Eq. (14) as

$$\alpha = \frac{\mathrm{e}^{-\lambda_{\mathrm{a}}l}}{\lambda_{\mathrm{a}} - \lambda_{\mathrm{b}}}[(f\lambda_{\mathrm{b}} + \xi)C_{\mathrm{b,e}} - (\lambda_{\mathrm{b}} + \zeta + \phi)C'_{\mathrm{a,e}}] \tag{20}$$

$$\beta = \frac{\mathrm{e}^{-\lambda_{\mathrm{b}}l}}{\lambda_{\mathrm{a}} - \lambda_{\mathrm{b}}}[-(f\lambda_{\mathrm{a}} + \xi)C_{\mathrm{b,e}} + (\lambda_{\mathrm{a}} + \zeta + \phi)C'_{\mathrm{a,e}}] \tag{21}$$

If inlet concentration $C_{\mathrm{a,i}}$ and the outlet concentration $C_{\mathrm{a,e}}$ are introduced into Eqs. (15) and (16), respectively, i.e.:

$$\text{At } x = 0: \quad C_{\mathrm{a},1} = C_{\mathrm{a,i}} \tag{22}$$

$$\text{At } x = 0: \quad C_{a,2} = C_{a,e} \tag{23}$$

one obtains, with the substitution of Eqs. (20) and (21):

$$C_{a,i} = AC_{b,e} - BC'_{a,e} \tag{24}$$

$$C_{a,e} = EC_{b,e} - FC'_{a,e} \tag{25}$$

where

$$A = \frac{(f\lambda_b + \xi)\,e^{-\lambda_a l} - (f\lambda_a + \xi)\,e^{-\lambda_b l}}{\lambda_a - \lambda_b} + f \tag{26}$$

$$B = \frac{(\lambda_b + \zeta + \phi)\,e^{-\lambda_a l} - (\lambda_a + \zeta + \phi)\,e^{-\lambda_b l}}{\lambda_a - \lambda_b} \tag{27}$$

$$E = \frac{1}{\phi}\left[\frac{-(\lambda_a + \zeta)(f\lambda_b + \xi)\,e^{-\lambda_a l} + (\lambda_b + \zeta)(f\lambda_a + \xi)\,e^{-\lambda_b l}}{\lambda_a - \lambda_b} + (\xi - \zeta f)\right] \tag{28}$$

$$F = \frac{1}{\phi}\left[\frac{-(\lambda_a + \zeta)(\lambda_b + \zeta + \phi)\,e^{-\lambda_a l} + (\lambda_b + \zeta)(\lambda_a + \zeta + \phi)\,e^{-\lambda_b l}}{\lambda_a - \lambda_b}\right] \tag{29}$$

Inspection of Eqs. (24) and (25) shows that the outlet concentrations, $C'_{a,e}$, $C_{a,e}$ and $C_{b,e}$, are not specified a priori. Mathematically, one more relation is needed for determination of these values. For this purpose, a mass balance for solute through the whole module is readily obtained as

$$C_{b,e} = C_{b,i} + \left(\frac{Q_a}{Q_b}\right)(C_{a,i} - C_{a,e}) \tag{30}$$

Solving Eqs. (24), (25) and (30), simultaneously, one has the outlet solute concentrations as

$$C_{a,e} = \frac{[FQ_b - (AF - BE)Q_a]C_{a,i} - [(AF - BE)Q_b]C_{b,i}}{(B - F)Q_b - (AF - BE)Q_a} \tag{31}$$

$$C_{b,e} = \frac{FC_{a,i} - (B - F)C_{a,e}}{AF - BE} \tag{32}$$

2.3. Mass-transfer rate

Once $C_{a,e}$ (or $C_{b,e}$) is calculated from Eq. (31) (or Eq. (32)), the total mass-transfer rate will be determined by Eq. (33), modified from Eq. (30):

$$W = Q_a(C_{a,i} - C_{a,e}) = Q_b(C_{b,e} - C_{b,i}) \tag{33}$$

3. Experiments

The chemicals, materials, dimensions of apparatus and experimental procedure are exactly the same as those employed and performed in previous work [12], except that in present experimental work, the impermeable plate of negligible thickness, instead of being placed at the centre line of channel a, was placed at arbitrary location and in vertical to the upper plate and the membrane sheet to divide channel a into two subchannels (subchannels a_1 and a_2) of height h and variable widths (i.e., $\Delta = 0.25$, 0.5 and 0.75), as shown in Fig. 1.

Experiments were carried out with the use of a membrane sheet ($l = w = 0.165$ m) made of microporous polypropylene(Gelman Sciences, average pore size = 0.2 μm, porosity = 70% and thickness = 178 μm) as a permeable barrier to extract acetic acid(reagent ACS grade, Fisher) from aqueous solution by methyl isobutyl ketone (MIBK, regent grade, Fisher). The membrane sheet was inserted in parallel between two parallel plates of stainless steel, with same distance from them to divide the conduit into two channels (channels a and b, or phases a and b) of same height ($h = 1.9 \times 10^{-3}$ m). Since microporous polypropylene is hydrophobic membrane, the organic solution (solute: acetic; solvent: MIBK) wets the membrane, and thus $H_{bc} = H_{bb} = 1$ and $H_{ac} = H_{ab} = 0.524$ at 25 °C [16]. A slight positive pressure (< 1 psig = 108 kPa) was maintained on the aqueous side of the apparatus to avoid breakthrough of the organic fluid.

4. Results and discussion

4.1. Comparison of theoretical predictions with experimental results

Many experimental data of various operating conditions for outlet solute concentration in phase a, $C_{a,e}$, were obtained [17] and the corresponding values of mass-transfer rate, W, were then calculated from Eq. (33). Some of the experimental results are plotted in Fig. 2.

It was found in previous work [12] that all overall mass-transfer coefficients vary linearly with Q_a, as well as with the fluid velocities, $v_{a,1}$ and $v_{a,2}$, in such small velocity range performed in present study, while over a larger range of velocities the mass-transfer coefficients actually vary with velocity to the one-third power [18]. The following correlation equations for K_1 (cocurrent flow) and K_2 (countercurrent flow) in terms of $v_{a,1}$ and $v_{a,2}$, respectively, were reached [12], applicable to the range of experimental conditions.

For $C_{a,i} = 5 \times 10^{-4}$ mol/cm^3:

$$K_1 \times 10^4\ (\text{cm/s}) = 3.865 + 1.484 v_{a,1} \tag{34}$$

$$K_2 \times 10^4\ (\text{cm/s}) = 5.016 + 0.718 v_{a,2} \tag{35}$$

For $C_{a,i} = 2.02 \times 10^{-3}$ mol/cm^3:

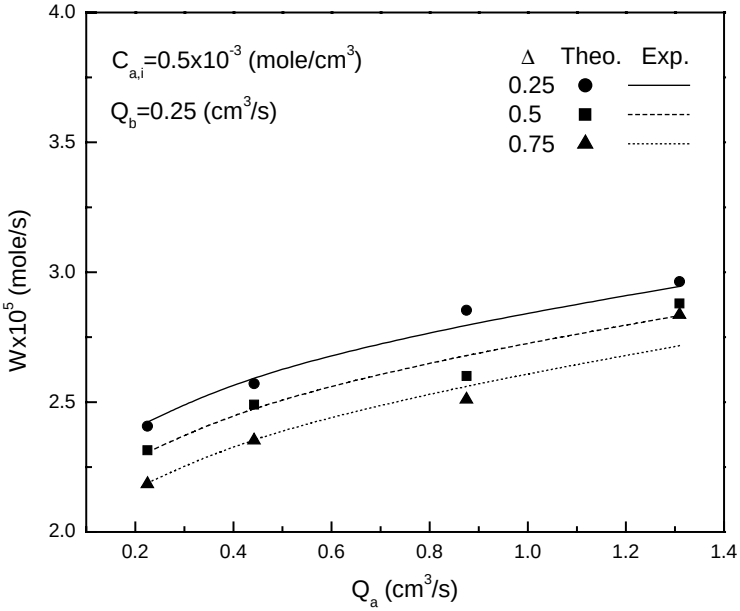

Fig. 2. Comparison of theoretical predictions with experimental results, $C_{a,i} = 0.5 \times 10^{-3}\,\mathrm{mol/cm^3}$, $Q_b = 0.25\,\mathrm{cm^3/s}$.

$$K_1 \times 10^4\,(\mathrm{cm/s}) = 2.152 + 0.846 v_{a,1} \quad (36)$$

$$K_2 \times 10^4\,(\mathrm{cm/s}) = 3.177 + 0.733 v_{a,2} \quad (37)$$

In Eqs. (34)–(37)

$$v_{a,1} = \frac{Q_a}{h \Delta w} \quad (38)$$

$$v_{a,2} = \frac{Q_a}{h(1-\Delta) w} \quad (39)$$

The theoretical predictions of mass-transfer rate were calculated from Eqs. (31) and (33) with the use of Eqs. (34)–(37), and some of them are also plotted in Figs. 2 and 3 for comparison. It is seen in these figures that the theoretical predictions for low flow rates are in good agreement with the experimental results, while those for higher flow rates are in qualitative agreement with, and rather larger than, the experimental results. This may be because that the assumption of uniform concentrations is not suitable for larger

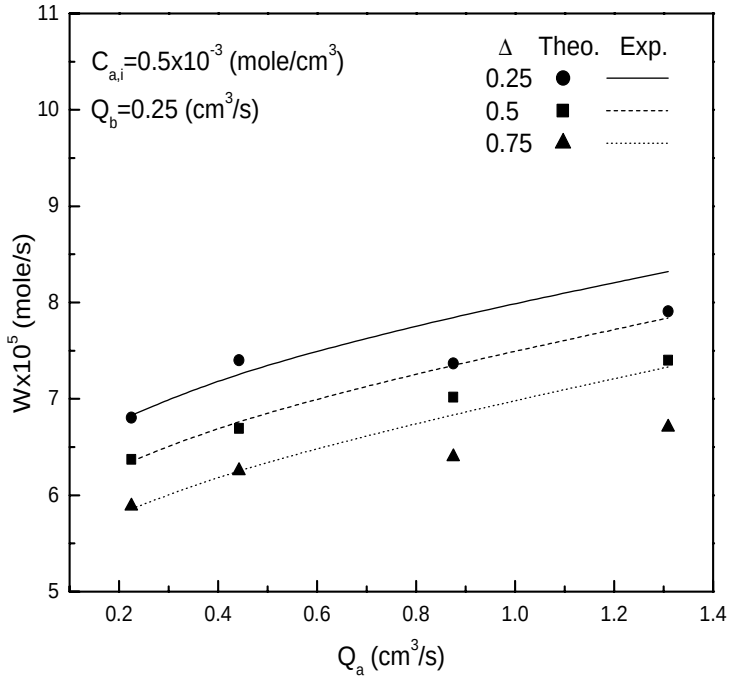

Fig. 3. Comparison of theoretical predictions with experimental results, $C_{a,i} = 2 \times 10^{-3}\,\mathrm{mol/cm^3}$, $Q_b = 0.25\,\mathrm{cm^3/s}$.

fluid velocities. It is also showed that W increases with Q_a, as well as with the decrease of subchannel-width ratio Δ.

4.2. Effect of Δ on mass-transfer rate

It is seen in Figs. 2 and 3 that the mass-transfer rate increases as the width of subchannel a_1, Δw, decreases (or the width of subchannel a_2 increases). This is because that for mass transfer, the countercurrent flow in subchannel a_2 is more effective than the cocurrent flow in subchannel a_1, and that larger mass-transfer area for countercurrent-flow channel is beneficial to total mass-transfer rate.

Tables 1 and 2 show the comparison of mass-transfer rate W obtained in the devices of $\Delta = 0.1$, 0.25 and 0.75 with that in the device of $\Delta = 0.5$ (with the impermeable plate placed at the centre line of raffinate phase) by the following definition:

$$I_W = \frac{W - W_{1/2}}{W_{1/2}} \tag{40}$$

where $W_{1/2}$ denotes the mass-transfer rate for $\Delta = 0.5$. It is seen in these tables that both positive and negative improvements in performance I_W based on $W_{1/2}$ gradually approach zero when the flow rate of raffinate phase Q_a increases. In other words, as Q_a increases the benefit of countercurrent-flow effect decreases. Therefore, under very high flow-rate operation the influence of channel-width ratio on the mass-transfer rate may be ignored. In this case, however, it is better to place the impermeable plate at the centre line for decreasing hydraulic dissipated power.

4.3. Effect of Δ on hydraulic dissipated power

In present study, an impermeable barrier with negligible thickness is placed vertically to the upper plate and membrane sheet, at an adjustable location of channel a (phase a) to divide the channel into two subchannels (subchannels a_1 and a_2) of widths Δw and $(1 - \Delta)w$ for double-pass operation. Though considerable improvement in mass transfer can be obtained by adjusting the location of barrier plate, the hydraulic dissipated power due to the friction loss of fluid flow should be discussed.

The hydraulic dissipated power in a parallel-plate channel may be estimated by

$$\begin{aligned} E &= (\text{fluid density} \times \text{volume flow rate}) \times \frac{\Delta P}{\text{fluid density}} \\ &= (\text{volume flow rate}) \times \Delta P \end{aligned} \tag{41}$$

If laminar flow in the flow channels is assumed, the pressure drop through the flow channel is [15]

$$\Delta P = \frac{12\mu l \times (\text{volume flow rate})}{h^2 \times (\text{cross-section area of channel})} \tag{42}$$

Since the total hydraulic dissipated power includes those in subchannel a_1, subchannel a_2 and channel b, we have

$$\begin{aligned} E &= E_{a,1} + E_{a,2} + E_b \\ &= \left[Q_a \frac{12\mu_a l Q_a}{h^3 \Delta w} \right] + \left[Q_a \frac{12\mu_a l Q_a}{h^3 (1-\Delta) w} \right] \\ &\quad + \left[Q_b \times \frac{12\mu_b l Q_b}{h^3 w} \right] \\ &= \frac{12l}{h^3 w} \left[\frac{\mu_a Q_a^2}{\Delta(1-\Delta)} + \mu_b Q_b^2 \right] \end{aligned} \tag{43}$$

The total hydraulic dissipated powers E for various operating conditions were calculated by Eq. (43) with $l = w = 16.5\,\text{cm}$, $h = 0.19\,\text{cm}$, $\mu_a = 1 \times 10^{-2}\,\text{g/cm s}$ and $\mu_b = 0.58 \times 10^{-2}\,\text{g/cm s}$. Let us define the enhancement of hydraulic dissipated power I_E based on $E_{1/2}$, the value of E obtained at $\Delta = 0.5$, as

$$I_E = \frac{E - E_{1/2}}{E_{1/2}} \tag{44}$$

Table 1
Predicting results with $C_{a,i} = 0.5 \times 10^{-3}\,\text{mol/cm}^3$, $Q_b = 0.25\,\text{cm}^3/\text{s}$ and $C_{b,i} = 0$

Q_a (cm^3/s)	$W_{1/2} \times 10^5$ (mol/s)	$E_{1/2} \times 10^9$ (hp)	I_W (%)			I_E (%)	
			$\Delta = 0.1$	$\Delta = 0.25$	$\Delta = 0.75$	$\Delta = 0.1$ or 0.9	$\Delta = 0.25$ or 0.75
0.1	1.992	0.06	8.58	5.32	−5.27	133	19
0.2	2.270	0.20	8.19	5.11	−5.15	165	30
0.4	2.468	0.76	7.66	4.82	−4.86	174	32
0.8	2.659	2.99	6.96	4.36	−4.48	177	33

Table 2
Predicting results with $C_{a,i} = 2.0 \times 10^{-3}\,\text{mol/cm}^3$, $Q_b = 0.25\,\text{cm}^3/\text{s}$ and $C_{b,i} = 0$

Q_a (cm^3/s)	$W_{1/2} \times 10^5$ (mol/s)	$E_{1/2} \times 10^9$ (hp)	I_W (%)			I_E (%)	
			$\Delta = 0.1$	$\Delta = 0.25$	$\Delta = 0.75$	$\Delta = 0.1$ or 0.9	$\Delta = 0.25$ or 0.75
0.1	5.706	0.06	12.63	7.94	−8.14	133	19
0.2	6.271	0.20	12.04	7.57	−7.77	165	30
0.4	6.729	0.76	11.76	7.40	−7.59	174	32
0.8	7.273	2.99	10.94	6.89	−7.08	177	33

Some of the results of I_E are also listed in Tables 1 and 2. It is shown in these tables that E and I_E increase when Δ goes far from 1/2 as well as when Q_a increases. However the hydraulic dissipated power is very small even for the system with extremely small Δ (or $1-\Delta$) and large Q_a where E is the largest. For instance, $E = 8.28 \times 10^{-9}$ hp for $\Delta = 0.1$ (or 0.9) and $Q_a = 0.8\,cm^3/s$. Therefore, the operating costs in the device of present interest may be ignored.

4.4. Opposite flow direction of phase b

There may exist another operation condition with phase b entering at $x = l$ and flowing in opposite direction. According, the fluids in the device flow concurrently first and then cocurrently within subchannels a_1 and a_2, respectively. In this case only the mass balance given in Eqs. (1) and (2) should be modified to

$$Q_b(C_b - C_{b,i}) = Q_a(C_{a,1} - C_{a,2}) \tag{45}$$

or

$$C_b = C_{b,i} + \left(\frac{Q_a}{Q_b}\right)(C_{a,1} - C_{a,2}) \tag{46}$$

The mathematical treatment and procedure as well as the results are the same as those performed in the device with fluids flowing cocurrently first and then countercurrently, except that Δ should be replaced by $(1-\Delta)$ [19].

5. Conclusion

The predicting equations for mass-transfer rate in double-pass parallel-plate membrane extractors of arbitrary barrier location, has been derived by mass balances. Experimental works were carried out in a stainless steel parallel conduit inserted with a membrane sheet made of microporous polypropylene to extract acetic acid from aqueous solution (phase a) by methyl iso-butyl ketone. Since the organic solution (phase b) wetted the membrane during operation, the membrane used in this study is hydrophobic. Theoretical predictions are qualitative agreement with the experimental results.

Considerable improvement in mass transfer can be achieved if the location of impermeable barrier for double pass is away from the centre line ($\Delta = 0.5$) with the manner that Δ (or $1-\Delta$) is set as small as possible for the flow pattern of cocurrent flow first and then countercurrent flow, while for the flow pattern of opposite directions, Δ is set as large as possible. Since the hydraulic dissipated powers are extremely small even operating with the change of the barrier location as shown in Tables 1 and 2, the operating cost in all devices may be ignored.

Acknowledgements

We wish to express our thanks to the National Science Council of ROC for financial aid under grant no. NSC-91-2214-E-032-001.

Nomenclature

A, B, E, F	constant defined by Eqs. (26)–(29)
C_a, C_b	bulk solute concentrations in phase a and in phase b (mol/cm^3)
$C_{a,e}, C_{b,e}$	outlet solute concentrations in phase a and in phase b (mol/cm^3)
$C_{a,i}, C_{b,i}$	inlet solute concentrations in phase a and phase b (mol/cm^3)
C_{a1}, C_{a2}	bulk solute concentrations in subchannel a_1 and subchannel a_2 of phase a (mol/cm^3)
$C'_{a,e}$	outlet concentrations in subchannel a_1, or inlet concentration in subchannel a_2 (mol/cm^3)
$C^0_{a,i}$	mixed inlet concentration in phase a (mol/cm^3)
E	hydraulic dissipated power (hp)
$E_{1/2}$	E obtained at $\Delta = 0.5$ (hp)
f	constant defined by Eq. (19)
h	half height of parallel channel, or distance between flat plate and membrane sheet (cm)
H_{ij}	distribution coefficient between phase i and phase j
I_E	enhancement of hydraulic dissipated power defined by Eq. (44)
I_W	improvement of mass-transfer rate, defined by Eq. (40)
K	average overall mass-transfer coefficient (cm/s)
K_1, K_2	K for cocurrent, and for countercurrent flow (cm/s)
l	the length of membrane sheet (cm)
ΔP	pressure drop in flow channel (N/cm^2)
Q_a, Q_b	inlet volume rates in phase a, and phase b (cm^3/s)
R	reflux ratio, reverse volume rate RQ_a divided by inlet volume rate Q_a
S	overall mass-transfer area of a flat-plate membrane module lw (cm^2)
$v_{a,1}, v_{a,2}$	fluid velocity in subchannel a_1, in subchannel a_2 (cm/s)
v_b	fluid velocity in phase b (cm/s)
w	width of membrane sheet (cm)
W	mass-transfer rate (mol/s)
$W_{1/2}$	W obtained at $\Delta = 0.5$ (mol/s)
x	axis along the flow direction

Greek letters

α	constant defined by Eq. (20)
β	constant defined by Eq. (21)
Δ	width ratio of subchannel a_1 to subchannel a_2
ε	porosity of membrane
ζ, ϕ, ξ	constant defined by Eqs. (8)–(10), respectively
λ_a, λ_b	constant defined by Eqs. (17) and (18), respectively
μ_a, μ_b	fluid viscosities of phase a and b, respectively (g/cm s)
τ	pore tortuosity of membrane
ω, η, θ	constant defined by Eqs. (11)–(13), respectively

References

[1] S.W. Tsai, H.M. Yeh, A study of the separation efficiency in horizontal thermal diffusion columns with external refluxes, Can. J. Chem. Eng. 63 (1985) 406.

[2] H.M. Yeh, S.W. Tsai, C.S. Lin, A study of the separation efficiency in thermal diffusion column with a vertical permeable barrier, AIChE J. 32 (1986) 971.

[3] H.M. Yeh, T.W. Cheng, S.W. Tsai, A study of the gratez problem in concentric-tube continuous-contact countercurrent separation processes with recycles at both ends, Sep. Sci. Technol. 21 (1986) 403.

[4] H.M. Yeh, S.W. Tsai, C.L. Chiang, Recycle effects on heat and mass transfer through a parallel-plate channel, AIChE J. 33 (1987) 1743.

[5] C.D. Ho, H.M. Yeh, W.S. Sheu, The analytical studies of heat and mass transfer through a parallel-plate channel with recycle, Int. J. Heat Mass Transfer 41 (1988) 2589.

[6] J. Korpijarvi, P. Oinas, J. Reunanen, Hydrodynamics and mass transfer in airlift reactor, Chem. Eng. Sci. 54 (1998) 2255.

[7] E. Santacesaria, M. Di Serio, P. Iengo, Mass transfer and kinetics in ethoxylation spray tower loop reactors, Chem. Eng. Sci. 54 (1999) 1499.

[8] E. Garcia-Calvo, A. Rodriguez, A. Prados, J. Klein, Fluid dynamic model for three-phase airlift reactors, Chem. Eng. Sci. 54 (1998) 2359.

[9] M. Stenas, M. Clark, V. Lazarova, Holdup and liquid circulation velocity in a rectangular air-lift bioreactor, Ind. Eng. Chem. Res. 38 (1999) 944.

[10] S. Goto, P.D. Gaspillo, Effect of static mixer on mass transfer in draft tube bubble column and in external loop column, Chem. Eng. Sci. 47 (1992) 3533.

[11] K.I. Kikuchi, H. Takahashi, Y. Takeda, F. Sugawara, Hydrodynamic behavior of single particles in a draft-tube bubble column, Can. J. Chem. Eng. 77 (1999) 573.

[12] H.M. Yeh, Y.Y. Peng, Y.K. Chen, Solvent extraction through a double-pass parallel-plate membrane channel with recycle, J. Membr. Sci. 163 (1999) 177.

[13] H.M. Yeh, C.H. Chen, Recycle effects on solvent extraction through concurrent-flow parallel-plate membrane modules, J. Membr. Sci. 190 (2001) 35.

[14] T.C. Lo, M.H.I. Baird, Liquid–liquid extraction, in: M. Grayson (Ed.), Kirktothmer Encyclopaedia of Chemical Technology, vol. 9, 3rd ed., Wiley, New York, 1980.

[15] R.B. Bird, W.E. Stewart, E.N. Lightfoot, Transport Phenomena, Wiley, New York, 1971, p. 62.

[16] H.M. Yeh, C.M. Huang, Solvent extraction in multipass parallel-flow mass exchangers of microporous hollow-fiber modules, J. Membr. Sci. 103 (1995) 135.

[17] C.H. Chen, The effect of various-type recycles on concurrent-flow solvent extraction in flat-plat membrane module, MS Thesis, Tamkang University, Tamsui, Taiwan, ROC, 2001.

[18] M.C. Poter, Handbook of Industrial Membrane Technology, Noyes Publications, New Jersey, 1990, pp. 1–3, 175.

[19] T.Y. Yueh, Effect of barrier location on solvent extraction in double-pass parallel-plate membrane modules, MS Thesis, Tamkang University, Tamsui, Taiwan, ROC, 2003.